Modeling the compositional dependence of electron diffraction in dilute GaAs- and GaP-based compound semiconductors

O. Rubel,* I. Németh, W. Stolz, and K. Volz
Department of Physics and Material Sciences Center, Philipps-University Marburg, Marburg 35032, Germany
(Received 26 November 2007; revised manuscript received 22 January 2008; published 25 August 2008)

The change in the intensity of the (200) electron-beam reflection induced by the incorporation of isovalent impurities in GaAs and GaP is studied theoretically. Calculations are performed in the framework of the kinematical scattering theory. The structure factor of random alloys was obtained using atomic form factors calculated with the density-functional theory and an empirical-potential valence force-field model for the structure relaxation. The calculations include the effect of redistribution of the electron density on the electron-scattering amplitudes as well as the effect of the local lattice distortions associated with the impurity sites. We propose a way to calculate these distortions analytically and to introduce them in a simple form to the expression for the structure factor. This method is an alternative to the simulations, which invoke demanding computations for atomic relaxation, and enables quantitative prediction of the compositional variation of the structure factor for dilute alloys taking into account static atomic displacements. The implications of the results for quantification of composition fluctuations in heterostructures using dark-field transmission electron microscopy are discussed. The effect of nitrogen and boron incorporation on the intensity of the (200) reflection is found to be partly compensated by the static atomic displacements they cause. Neglecting this effect would lead to an underestimation of the impurity content by approximately a factor of two. The redistribution of the electron density is found to be less crucial for the evaluation of the chemical composition leading to a relative error in the (200) scattering amplitude of about 16%.

DOI: 10.1103/PhysRevB.78.075207 PACS number(s): 61.05.jd, 61.66.Dk, 71.15.Mb, 68.37.Lp

I. INTRODUCTION

III-V compound semiconductors provide the material basis for a number of electronic and optoelectronic applications. Alloying of semiconductors by isoelectronic substitutional atoms is used in order to tune their energy gap and/or lattice constant to a desirable value.[1–3] The quality of such mixed crystals is strongly dependent on the homogeneity of the distribution of the chemical constituents. Cross-sectional dark-field transmission electron microscopy (DF-TEM) provides a unique opportunity to access the chemical composition of the structures on the nanoscale.[4–7]

The chemical information on zinc-blende III-V compound semiconductors can be obtained by studying the intensity of the (200) reflection. According to the kinematic scattering theory, the intensity of a beam diffracted by planes $\mathbf{g}=(h,k,l)$ is proportional to the square of the corresponding structure factor, i.e., $I(\mathbf{g}) \propto |F(\mathbf{g})|^2$. The simplest way to calculate the structure factor of solid solutions is to use the virtual-crystal approximation, which implies the position of atoms to be unperturbed with respect to the average crystal sites. Accordingly, the compositional dependence of the (200) structure factor in a zinc-blende ternary $AB_{1-x}C_x$ alloy (reduced to the two-atom basis) has the form

$$F(200) \approx xf(\mathrm{C}) + (1-x)f(\mathrm{B}) - f(\mathrm{A}), \tag{1}$$

where f's are the electron-scattering factors for individual chemical species.

Glas *et al.*[8,9] showed that the validity of Eq. (1) is limited to the case when the substitutional constituencies do not introduce significant local distortions of the atomic positions. Otherwise, it is necessary to include static atomic displacements, which can be calculated by computer simulations using an empirical-potential method.[8,9] This concept was experimentally verified by measurement of the (200) DF-TEM intensity of dilute $GaAs_{1-x}N_x/GaAs$ quantum wells.[10] This experiment demonstrated that the local lattice distortions caused by nitrogen have a significant impact on the (200) DF-TEM intensity and should be taken into account if quantitative estimate of the nitrogen content is the aim.

Taking into account the actual distribution of the electron density in solids enables further improvement of the accuracy, with which the structure factor can be computed.[11,12] Instead of form factors for isolated atoms, Rosenauer *et al.*[12] suggested using the so-called modified atomic scattering amplitudes calculated *ab initio* for each solid solution under consideration. However, such data for most III-V compounds are lacking.

Here we present a comprehensive theoretical study of the compositional dependence of the (200) electron-scattering intensity in dilute $GaAs_{1-x}N_x$, $GaP_{1-x}N_x$, $Ga_{1-x}B_xAs$, $Ga_{1-x}B_xP$, $GaAs_{1-x}Sb_x$, and $GaP_{1-x}As_x$ semiconductor alloys. Calculations are carried out using the density-functional theory (DFT) for the complete structure factor evaluation and also using Keating's valence force-field (VFF) model[13] for the structure relaxation in conjunction with the atomic form factors calculated using DFT. Both methods take into account effects of the static atomic displacements caused by substitutional impurities and redistribution of the electron density due to the formation of chemical bonds. We thoroughly inspect the accuracy of VFF for the structure relaxation by comparing to the results of DFT. A general expression for local lattice distortions caused by substitutional impurities in zinc-blende solids is obtained on the base of the VFF strain energy functional. In a dilute impurity limit, the correction to the structure factor calculation for the associ-

ated lattice distortions can be introduced as an additional factor to the last term in Eq. (1). This enables one to calculate *analytically* the compositional dependence of the structure factor for an arbitrary alloy, taking into account static atomic displacements.

II. COMPUTATIONAL DETAILS

The structure factor calculations for GaAs- and GaP-based ternary alloys are performed, combining the methods suggested in Refs. 9 and 12. We consider a zinc-blende 27000-atom supercell with periodical boundary conditions, which shows an adequate convergence for the structure factor. The alloy is generated by *random* distribution of the substitutional impurity atoms (B, N, P, As, or Sb) with the concentration x in the corresponding sublattice. Effect of the epitaxial strain is included as described in Ref. 12 by setting up the lattice constant in the lateral directions ([100] and [010]) to that of the substrate (i.e., GaP or GaAs) and altering the lattice constant in the "growth direction" according to the chemical composition of the alloy under consideration. As a result of the macroscopic strain, planes parallel and perpendicular to the "growth direction" become nonequivalent that causes differences in the scattering intensity. This issue was investigated in Ref. 10 where no remarkable difference in the intensity of beams scattered by {200} planes parallel and perpendicular to the growth direction was found for dilute $GaAs_{1-x}N_x/GaAs$ quantum wells. In the following we discuss scattering by (200) planes, i.e., those parallel to the growth direction, since in that case the interplane distance (and therefore the scattering angle) is independent of the chemical composition. Such a strain state is justified when the TEM sample thickness is much greater than the thickness of the alloy layer under investigation. Otherwise, relaxation effects should be taken into account.[12] In the supercell, all atoms are first placed at their ideal (unperturbed) positions and then relaxed using VFF, keeping the macroscopic strain unchanged. The structure factor for an arbitrary reflection $\mathbf{g}$ is calculated from

$$F(\mathbf{g}) = \sum_j f_j \exp(i2\pi \mathbf{g} \cdot \boldsymbol{\rho}_j), \tag{2}$$

where $\boldsymbol{\rho}_j$ is the vector of fractional coordinates corresponding to the atom labeled j. The atom form factors are calculated using DFT as described below.

A. Valence force field

The positions of the atoms in the supercell are optimized using Keating[13] VFF model generalized for zinc-blende mixed crystals.[14] Atomic coordinates are found by minimizing the total strain energy of the supercell $\Sigma_s E_{\text{strain}}(\mathbf{r}_s)$, where $E_{\text{strain}}(\mathbf{r}_s)$ denotes the individual contribution of atom s. The strain energy per atom is given by the functional[13,14]

TABLE I. Force-field parameters (α, β) and equilibrium bond length (r_0) for the zinc-blende binary solids.

Compound	α (N/m)	β (N/m)	r_0 (nm)
GaAs	39.46	9.30	0.24479
GaP	44.49	10.70	0.23601
GaN	81.4	17.1	0.19572
GaSb	31.84	7.33	0.26396
BAs	62.88	23.84	0.20513
BP	69.27	30.59	0.19477

$$E_{\text{strain}}(\mathbf{r}_s) = \frac{1}{4}\sum_{i=1}^{4} \frac{3}{4r_{0_{si}}^2}\alpha_{si}(\mathbf{r}_{si}\cdot\mathbf{r}_{si} - r_{0_{si}}^2)^2 + \frac{1}{4}\sum_{i=1}^{4}\sum_{\substack{j=1 \\ j\neq i}}^{4} \frac{3}{4r_{0_{si}}r_{0_{sj}}}\beta_{isj}(\mathbf{r}_{si}\cdot\mathbf{r}_{sj} - r_{0_{si}}r_{0_{sj}}\cos\theta_{0_{isj}})^2, \tag{3}$$

where s, i, and j are the atomic labels, r_0 is the equilibrium interatomic distance, θ_0 is the equilibrium bond angle, $\mathbf{r}_{si} = \mathbf{r}_s - \mathbf{r}_i$ is the relative position vector of the atomic species, and α and β are the force constants, which are related to the stiffness constants of the binary solids. The summation indexes i and j in Eq. (3) run over the first nearest neighbors of the atom s. For asymmetrical bonds, i.e., when the chemical species i and j are not identical, the bond-bending force constant β_{isj} is determined by the averaging procedure $\beta_{isj} = (\beta_{isi} + \beta_{jsj})/2$.[15,16]

Force-field parameters for the compounds studied here are listed in Table I. The parameters for GaAs, GaSb, and GaP were determined from experimental values[2] of the stiffness coefficients and the lattice constant using the following relations:[13]

$$\alpha = \frac{r_0}{\sqrt{3}}(C_{11} + 3C_{12}), \tag{4a}$$

$$\beta = \frac{r_0}{\sqrt{3}}(C_{11} - C_{12}), \tag{4b}$$

For the zinc-blende GaN, we use the force-field parameters suggested in Ref. 16. Because of the large uncertainty in elastic properties reported in the literature for BAs and BP, we first calculated the lattice constant and the elastic properties of BAs and BP using DFT and then determined the force constants using Eqs. (4a) and (4b). According to the calculations, BAs has the following properties: $C_{11}=284$ GPa, $C_{12}=82$ GPa, and $a_0=0.47373$ nm. The corresponding results for BP are: $C_{11}=358$ GPa, $C_{12}=86$ GPa, and $a_0=0.4497$ nm. The theoretical values for the lattice constant of borides are about 1% less than the corresponding experimental values,[17] which is typical for DFT with the local-density approximation.

B. Density-functional theory

DFT is used in order to relax atomic positions and to calculate electron-scattering factors for individual atoms in a small supercell. Calculations are carried out in the framework of the full-potential linearized augmented plane-wave method using WIEN2K software package.[18] We restrict the calculations to the 64-atom cubic supercells with periodical boundary conditions. The impurity is introduced by substitution of a single atom in the host (GaAs or GaP) supercell with one of the following species: B, N, P, As, or Sb. The lattice constant was kept at the equilibrium DFT value of GaAs or of GaP. The atomic position were optimized and the converged distribution of the charge density was obtained.

In the calculations, we use the local-density approximation[19] for the exchange-correlation functional. The energy to separate core and valence electrons was set to −6 Ry. This makes the treatment of $3d$-Ga electrons as valence electrons possible, which is important for nitrides.[20] The Brillouin zone of 64-atom supercell was sampled using $4\times4\times4$ shifted Monkhorst-Pack k-point mesh.[21] The volume of the supercell was partitioned onto nonoverlapping spheres centered at the nucleus of the individual atoms. The radii of the spheres have the following values (in bohr) depending on the chemical element at which they are centered: $R(\mathrm{B})=1.65$, $R(\mathrm{N})=1.68$, $R(\mathrm{P})=2.0$, $R(\mathrm{Ga})=2.0$, $R(\mathrm{As})=2.0$, and $R(\mathrm{Sb})=2.2$. The product of the smallest of all atomic sphere radii in the supercell and of the plane-wave cutoff in k space (the so-called $RK_{\max}$ parameter) was equal to 7 for all compositions. This corresponds to the cut-off energy of about 12–18 Ry, depending on the atomic species involved. The structural optimization was continued until the forces acting on the atoms did not fall below 2 mRy/bohr.

After performing the structural optimization and obtaining the converged charge density, the x-ray structure factor is calculated using the LAPW3 routine of WIEN2K.[18] The x-ray structure factor can be split to the contribution of each individual atomic sphere $f_{x_j}^{(\mathrm{inner})}$ and of the interstitial region $f_x^{(\mathrm{out})}$. The part of the structure factor, which belongs to the interstitial region of the supercell, is equally distributed among other atoms such that the x-ray atomic form factor takes the form[12]

$$f_{x_j}=f_{x_j}^{(\mathrm{inner})}+f_x^{(\mathrm{out})}/n, \tag{5}$$

where n is the number of atoms in the supercell, i.e., 64 in our case. The x-ray scattering factors f_x are converted to the electron-scattering factors using the Mott-Bethe relationship,[22]

$$f=\frac{me^2}{8\pi\epsilon_0h^2s^2}(Z-f_x), \tag{6}$$

where m is the electron mass, e is the elementary charge, h is the Planck's constant, ϵ_0 is the permittivity of free space, $s=1/2d$ with d being the spacing between diffracting planes $\mathbf{g}$, and Z is the atomic number. The values of $f_{x_j}^{(\mathrm{inner})}$ calculated by WIEN2K include the relaxed atomic positions due to the phase factor $\exp(i2\pi\mathbf{g}\cdot\boldsymbol{\rho}_j)$, which is implicitly present in $f_{x_j}^{(\mathrm{inner})}$ and should be subtracted before applying Eq. (6).

III. RESULTS AND DISCUSSION

In Sec. I we have pointed out two factors, which are necessary to consider in order to achieve an accurate value of the structure factor and, thus, of the electron-scattering intensity. These factors are (i) the static atomic displacements caused by substitutional impurities and (ii) redistribution of the electron density due to the formation of chemical bonds. Both can be calculated self-consistently using DFT. We consider substitution of a single atom in a 64-atom periodic supercell that forms an ordered alloy with the concentration of impurity atoms of about 3%. After iterative minimization of the total energy, one obtains the ground-state charge distribution and relaxed position of the nuclei. Then, the electron structure factor is calculated from

$$F=\frac{me^2}{8\pi\epsilon_0h^2s^2}(\mathcal{Z}-F_x) \tag{7}$$

using the DFT x-ray structure factor F_x for the whole supercell, calculated by the Fourier transformation of the charge density, and the nucleus charge modified by the phase factor,

$$\mathcal{Z}=\sum_j Z_j\exp(i2\pi\mathbf{g}\cdot\boldsymbol{\rho}_j). \tag{8}$$

This approach, referred below as "full DFT," provides the most accurate results for the structure factor (except for the Debye-Waller correction neglected here), which will be used as a reference for less strict approaches. The corresponding results for the normalized (200) electron-scattering intensity in several compounds are shown in Fig. 1 by cross symbols.

Unfortunately, the full DFT approach is restricted to a relatively small size of the supercell, which is inappropriate for studying random alloys. In order to overcome this limitation, we use another method of the structure factor calculation. It is based on the combination of the atomic form factors calculated using DFT and the atomic structure relaxation performed using Keating's VFF model. In this method, the form factors are calculated *ab initio* once for each atomic species in a particular environment and then treated as constants. This reduces the computational efforts dramatically and enables calculation of the structure factor for supercells with thousands of atoms.

Prior to the application of the VFF to the structure relaxation, we verify the accuracy of this approach. For this purpose, we calculate the bond length of single substitutional impurities in GaAs and in GaP cubic 64-atom supercells using DFT and VFF. The bond distortion of the host crystal associated with the impurity atom is characterized by the strain

$$\epsilon=(r-r_0)/r_0, \tag{9}$$

where r is the relaxed anion-cation bond length at the impurity site and r_0 is the equilibrium anion-cation bond length for the host crystal, i.e., that of GaAs or of GaP in our case. A similar test has been performed for GaAs:N and GaP:N (Ref. 23) as well as for GaAs:B,[24] confirming the accuracy of VFF. We extend this test to a variety of III-V compounds studied here. The corresponding bond distortions are listed in Table II along with the results of previous studies. Consis-

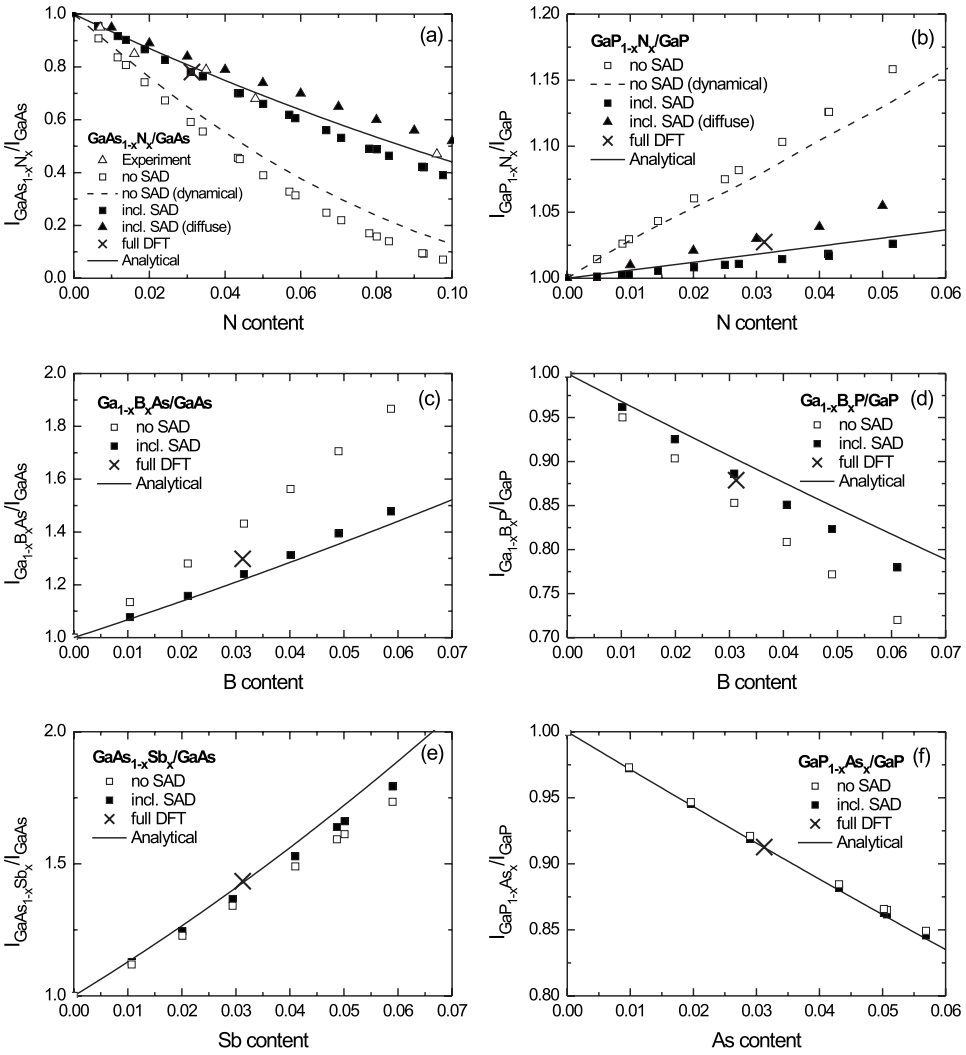

FIG. 1. Compositional dependence of the (200) electron-beam intensity in ternary III-V semiconductor alloys calculated using the virtual-crystal approximation (□) and including static atomic displacements (SAD) for large supercells (■). Experimental results for $GaAs_{1-x}N_x/GaAs$ quantum wells (Ref. 10) are shown by open triangles on panel (a). The solid line shows results of Eqs. (12) and (13), which include the effect of atomic displacements in a simplified way. Atomic form factors calculated using DFT are taken from Table III. Results of the *ab initio* calculations for a single impurity in the 64-atom supercell are shown by crosses. Results of the dynamical theory for the acceleration voltage of 300 kV and the sample thickness of 50 nm obtained assuming the virtual-crystal approximation are shown on panels (a) and (b) by dashed lines. The compositional variation of the relative intensities, which additionally takes into account diffuse scattering, are shown on panels (a) and (b).

tency between the bond strains calculated using DFT and VFF gives confidence in VFF for the structure relaxation.

In the following, we analyze the compositional dependence of the (200) electron-scattering intensity in GaAs- and GaP-based ternary alloys. Electron form factors for various atomic species (B, N, As, P, and Sb) substituted in GaAs and in GaP are listed in Table III along with the corresponding results for isolated atoms, shown for reference. The structure factor of ternary semiconductor alloys is calculated using bulk values of the form factors from Table III and atomic positions determined by VFF. The corresponding normalized (200) electron-scattering intensity is shown in Fig. 1 (filled symbols) as a function of the impurity content. These results agree well with those obtained using the self-consistent full DFT approach (Fig. 1, cross symbols). Furthermore, we show in Fig. 1(a) the experimental data for the relative compositional variation of the (200) DF-TEM intensity in $GaAs_{1-x}N_x/GaAs$ quantum wells taken from Ref. 10. The agreement between theoretical and experimental data is excellent. This confirms that VFF relaxation of atomic positions in conjunction with the DFT form factors provides accurate values of the structure factor for III-V solid solutions.

In order to highlight the role of atomic displacements, we also calculate variation of the intensity using the virtual-

TABLE II. Strain of anion-cation bond lengths around isolated isovalent impurities in GaAs and in GaP cubic 64-atom supercells relative to the bond length of the host crystal calculated using various approaches. MZ refers to the analytical expression proposed by Martins and Zunger (Ref. 14) based on the VFF model; BO corresponds to the bond orbital model of Shen (Ref. 26).

Compound	DFT	VFF	Equation (13)	MZ	BO
GaAs:N[a]	−0.155	−0.158	−0.141	−0.158	…
GaAs:B[b]	−0.113	−0.117	−0.115	−0.120	…
GaAs:Sb	+0.053	+0.050	+0.058	+0.046	+0.057
GaAs:P[c]	−0.025	−0.025	−0.027	−0.024	−0.025
GaP:Sb	+0.082	+0.072	+0.086	+0.066	+0.089
GaP:As[d]	+0.025	+0.023	+0.027	+0.023	+0.027
GaP:N[e]	−0.127	−0.132	−0.122	−0.130	…
GaP:B	−0.122	−0.124	−0.122	−0.128	…

[a]Previous studies: −0.151 (DFT, Ref. 23).
[b]−0.114 and −0.127 (DFT and VFF, respectively, Ref. 24).
[c]−0.029 (VFF, Ref. 30).
[d]+0.025 (VFF, Ref. 30).
[e]−0.137 (DFT, Ref. 23).

TABLE III. Kinematic (200) electron form factors (Å) for various chemical species calculated using DFT for GaAs- and GaP-based solid solutions and the corresponding values for isolated atoms calculated by Doyle and Turner (Ref. 31). In order to include the relativistic correction for electrons of velocity v, these values should be multiplied by $(1-v^2/c^2)^{-1/2}$, where c is the velocity of light in vacuum.

Compound	Ga	As	P	N	Sb	B
Calculated for bulk						
GaAs:X	3.97[a]	4.34[b]	3.00	1.52	6.37	1.58
GaP:X	3.81	4.17	2.86	1.45	6.15	1.45
Data for isolated atoms						
GaAs:X	4.00	4.45	3.14	1.58	6.59	1.56
GaP:X	3.89	4.33	3.04	1.54	6.42	1.50

[a]Previous study: 3.87 Å (Ref. 12).
[b]4.25 Å (Ref. 12).

crystal approximation (Fig. 1, open symbols). This dependence has a parabolic form since it is governed by the square of the structure factor given by Eq. (1). The most pronounced effect of atomic displacements is observed for nitrogen- and boron-containing alloys, since these two elements cause relatively large lattice distortions (see Table II). For antimony- and arsenic-doped alloys, the changes introduced by atomic displacements are negligible.

In addition, we investigate the effect of atomic displacement on diffuse scattering, which leads to smearing of the diffraction pattern. This effect was investigated by Glas,[25] albeit not for the (200) reflection. The diffraction pattern of $GaAs_{1-x}N_x$ and $GaP_{1-x}N_x$ alloys was calculated using a methodics described in Ref. 8. The intensity was integrated in the reciprocal space including not only (200) reflection but also closely adjacent reflections located from (200) not farther than the half of the distance between (200) and (000) in the reciprocal space. Results of the calculations are shown in Fig. 1. Apparently, the diffuse scattering results in higher integral intensity. The effect becomes pronounced with increasing the impurity content. In the case of $GaAs_{0.9}N_{0.1}$ alloy, contribution of the diffuse scattering to the integral (200) intensity is about 10%, whereas the corresponding value for $GaP_{0.95}N_{0.05}$ alloy is only 1%, which is certainly below the error bar of experimental measurements. To gain further insight to the role of atomic displacements in the structure factor calculations, we develop a simplified approach that enables analytical calculation of the structure factor of an alloy in the dilute limit.

Let us consider an arbitrary ternary alloy $AB_{1-x}C_x$ with $x \to 0$. In this limit, one can neglect the interaction between substitutional atoms C and regard each of them acting as an isolated impurity. Further on, we assume that the relaxation occurs only by displacing atoms in the first nearest-neighbor shell around the impurity atoms (Fig. 2). Thus, the concentration of the displaced atoms will be $4x$, since all atoms are fourfold coordinated. All other atoms remain at their unperturbed position $\boldsymbol{\rho}_0$ in accordance with the assumption above. Under such circumstances, the structure factor of this alloy reduced to the two-atom basis can be written in the form

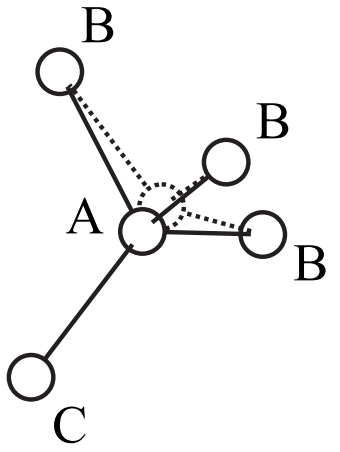

FIG. 2. Local bond configuration of isolated substitutional atom C in zinc-blende AB host crystal. Dotted lines correspond to the unrelaxed bond configuration.

$$F(\mathbf{g}) = xf(\mathrm{C}) + (1-x)f(\mathrm{B}) + (1-4x)f(\mathrm{A})\cos(2\pi\mathbf{g}\cdot\boldsymbol{\rho}_0) + 4xf(\mathrm{A})\cos[2\pi(1+\epsilon)\mathbf{g}\cdot\boldsymbol{\rho}_0], \quad (10)$$

where ϵ is the bond distortion introduced by the impurity atom as defined by Eq. (9). Owing to the inequality $\epsilon \ll 1$, one can simplify Eq. (10) using a series expansion[9] and express the structure factor as

$$F(\mathbf{g}) \approx xf(\mathrm{C}) + (1-x)f(\mathrm{B}) + [1-8x(\pi\epsilon\mathbf{g}\cdot\boldsymbol{\rho}_0)^2]f(\mathrm{A})\cos(2\pi\mathbf{g}\cdot\boldsymbol{\rho}_0). \quad (11)$$

For the chemical-sensitive (200) reflection, the structure factor takes the form

$$F(200) \approx xf(\mathrm{C}) + (1-x)f(\mathrm{B}) - [1-2x(\pi\epsilon)^2]f(\mathrm{A}). \quad (12)$$

The obtained form of the structure factor is very similar to Eq. (1) for the virtual-crystal approximation. The only difference between Eqs. (1) and (12) is the additional factor $2x(\pi\epsilon)^2$, which accounts for the atomic displacements caused by the substitutional atoms C and vanishes if $\epsilon=0$.

Equation (11) enables analytical calculation of the structure factor for dilute alloys instead of performing elaborate supercell simulations. The bond strain ϵ required for the calculations can be obtained either by DFT or by VFF calculations (see Table II). Alternatively, we propose an approximate analytical expression, which is intended to provide a crude estimate for ϵ. This expression is derived for the lattice distortion around the isolated impurity atom C substituted at the place of atom B in the host crystal AB (see Appendix). By minimizing the VFF strain energy functional, one obtains the optimal bond strain,

$$\epsilon \approx \frac{3\alpha_{\mathrm{AC}}(r_{0_{\mathrm{AC}}}^2 - r_{0_{\mathrm{AB}}}^2)}{(2\alpha_{\mathrm{AB}} - 3\alpha_{\mathrm{AC}})r_{0_{\mathrm{AC}}}^2 + 9\alpha_{\mathrm{AC}}r_{0_{\mathrm{AB}}}^2} \quad (13)$$

as a function of the conventional VFF parameters. Results predicted by Eq. (13) are presented in Table II along with the DFT and VFF data for comparison. In spite of the number of approximations involved in Eq. (13), it gives indeed suffi-

ciently accurate values of strain for all compounds studied here. In addition we show in Table II the results for the bond strain obtained using two alternative approaches proposed by Martins and Zunger[14] and by Shen.[26] For the compounds studied here, the results of Martins and Zunger[14] have a twice larger average relative error than the results of Eq. (13).

Now we combine the simplified expression for the structure factor [Eq. (12)] with the expression for the bond strain [Eq. (13)] and calculate the relative change of the (200) electron-scattering intensity in ternary alloys analytically. Results are shown in Fig. 1 by solid lines. As one can see, the calculated intensity is in good agreement with VFF calculations for large supercells. Some deviations can be attributed to the isolated impurity approximation, which is the central assumption in Eqs. (10)–(13). The isolated impurity approximation is valid when the probability that there is an impurity atom in the second shell around the central impurity approaches zero. Such a probability significantly deviates from zero even for the concentration of impurity atoms of a few percent. In that case pairs of impurities are formed that influences the atomic positions and (even more important) the number of atoms involved in the relaxation. When such a pair is formed, i.e., two impurity atoms are bonded to one atom, the number of displaced atoms reduces by one as compared to the case of the isolated impurities. As a result, the isolated impurity approximation tends to overestimate the effect of impurities on the DF-TEM intensity (as one can see from Fig. 1) and should be used with care. Despite of that, Eq. (11) has a clear advantage over the virtual-crystal approximation (at least for the range of alloy concentrations studied here) (see Fig. 1) and includes dominant effects of atomic displacements in the simplest form. Taking advantage of the analytical form of Eq. (11), one can readily apply it for DF-TEM image analysis.

Dark-field images taken with (200) diffraction spot are usually used in order to judge on homogeneity of distribution of the chemical constituents (see, e.g., Ref. 27, p. 538). Sensitivity of a particular reflection to the variation of the chemical compositions can be characterized by the bowing parameter defined as

$$b = \frac{\partial}{\partial x}\left(\frac{I_{\mathrm{AB}_{1-x}\mathrm{C}_x}}{I_{\mathrm{AB}}}\right). \tag{14}$$

The larger the value of $|b|$, the more sensitive the contrast variation to the compositional fluctuations. In the range of applicability of Eq. (12), i.e., for $x \to 0$, the compositional bowing parameter for (200) reflection can be written in the form

$$b(200) \approx \frac{2f(\mathrm{C}) - 2f(\mathrm{B}) + 4(\pi\epsilon)^2 f(\mathrm{A})}{f(\mathrm{B}) - f(\mathrm{A})}. \tag{15}$$

Now we can see how crucial the effect of static atomic displacements and of electron redistribution is for the slope of the contrast variation. For this purpose, we calculate the (200) bowing parameter using Eq. (15) with different values for the form factors f and for the strain ϵ. Results are summarized in Fig. 3 for the variety of alloys. Apparently, the

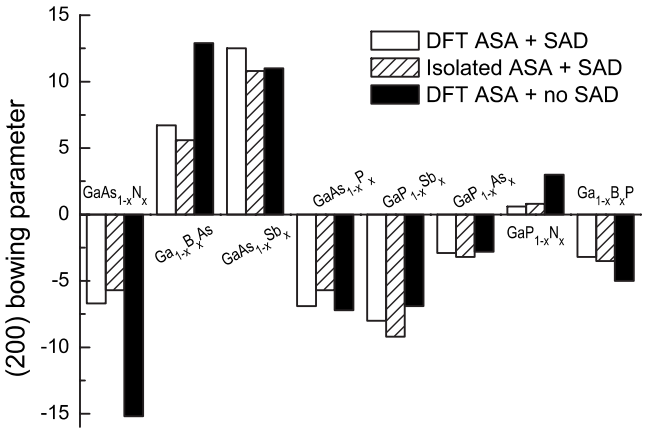

FIG. 3. Compositional bowing parameter for the (200) electron-scattering intensity in various III-V ternary alloys. Results are calculated using Eq. (15) assuming different input parameters for the atomic scattering amplitudes (ASA) from Table III. In the calculations, the local bond strain ϵ associated with the static atomic displacements (SAD) is either determined using Eq. (13) or assumed to be zero in the case labeled as "no SAD."

sensitivity of the (200) reflection to the variation of the chemical composition strongly depends on the correspondence between form factors of the constituencies involved. The atomic displacements also have a significant impact on the accuracy, with which the compositional bowing is calculated. For instance, $GaP_{1-x}N_x$ shows practically no compositional variation of the (200) intensity, since the effect of nitrogen is neutralized by the static displacements it causes. Redistribution of the electron density plays, however, a secondary role in determining the compositional bowing of (200) intensity and becomes the most important factor in the case of alloying with heavier elements, such as P, As, and Sb, which is also evident from the study of $Ga_{1-x}In_xAs$ alloys.[12]

Finally, we would like to comment on the application of the theoretical results discussed here to experimental measurements performed for samples of a finite thickness. DF-TEM images are usually taken under the so-called two-beam excitation conditions (Ref. 27, p. 361), i.e., when only one set of Bragg reflecting planes, (200) in our case, is at the reflecting position. Under such circumstances, the kinematical theory of diffraction used here breaks down as the TEM foil thickness measured in the direction of the incident beam approaches the critical value of $\xi(\mathbf{g})/\pi$ (Ref. 28, p. 195), where $\xi(\mathbf{g})$ is the extinction length corresponding to the reflection $\mathbf{g}$. For the (200) reflection and electrons with the energy of 300 keV, this critical thickness in GaAs and GaP is 390 and 140 nm, respectively. The thickness of samples used in experiments for dark-field imaging is usually much less than the critical thickness (typically between 30 and 50 nm). Therefore, the results of the kinematical theory can be trusted. In order to strengthen our arguments further, we show in Figs. 1(a) and 1(b) the results for the relative compositional variation of the (200) intensity in $GaAs_{1-x}N_x$ and $GaP_{1-x}N_x$ alloys calculated using the EMS software package[29] in the framework of the dynamical theory (Bloch waves) and the virtual-crystal approximation for the sample thickness of 50 nm, the acceleration voltage of 300 kV, and the two-beam

excitation conditions by having the center of Laue circle at (1.5 0 20). These data are in good agreement with the corresponding results of the kinematical theory [open squares in Figs. 1(a) and 1(b)], which gives confidence to other theoretical predictions reported in the paper.

IV. CONCLUSIONS

The compositional dependence of the (200) electron-diffraction intensity in epitaxial thin layers of dilute $GaAs_{1-x}N_x$, $GaP_{1-x}N_x$, $Ga_{1-x}B_xAs$, $Ga_{1-x}B_xP$, $GaAs_{1-x}Sb_x$, and $GaP_{1-x}As_x$ semiconductor alloys was studied theoretically. Calculations are performed in the framework of the kinematical scattering theory, i.e., assuming that the scattering intensity is proportional to the square of the corresponding structure factor. The structure factor of random alloys was obtained using atomic form factors calculated with the density-functional theory (DFT) and an empirical-potential valence force-field (VFF) model for the structure relaxation. The accuracy of the VFF model for the structure relaxation is examined for a variety of compounds and an excellent agreement with the results of DFT was found. Obtained results for the intensity of (200) reflection agreed well with the full *ab initio* calculations for small supercells. This signifies that the calculations accurately incorporate effects of the local lattice distortions caused by impurity atoms as well as redistribution of the electron density due to the formation of chemical bonds. The static atomic displacements caused by substitutional impurities are found to have a major influence on the scattering intensity in nitrogen- and boron-containing alloys. It was shown that, in the impurity limit, the atomic displacements can be introduced as a correction term to the expression for the structure factor obtained in the framework of the virtual-crystal approximation. This correction term explicitly includes the bond distortion, which can be calculated analytically using the expression suggested. Neglecting the effect of static atomic displacements leads to an underestimate of the impurity content in $GaAs_{1-x}N_x$, $GaP_{1-x}N_x$, and $Ga_{1-x}B_xAs$ alloys by approximately a factor of two. The redistribution of the electron density is found to be less crucial for evaluation of the chemical composition leading to a relative error in the (200) scattering amplitude of about 16%.

ACKNOWLEDGMENTS

Financial support of the German Science Foundation in the framework of the topical research group "Metastable Compound Semiconductors and Heterostructures" as well as in the framework of the European Graduated College "Electron-Electron Interactions in Solids," the European Community [IP "FULLSPECTRUM" Ref. No. SES6-CT-2003-502620)], and the Optodynamic Center at the Philipps-University Marburg are gratefully acknowledged.

APPENDIX

Here we calculate the local distortion of bonds associated with the isolated substitutional impurity atom C in the zinc-blende lattice of atoms A and B. The local configuration of bonds is shown in Fig. 2. It is assumed that the relaxation takes place only in the nearest-neighbor shell, i.e., by changing the length of A-C bonds. This implies that the position of atom B remains unchanged during the relaxation. According to the VFF energy functional given by Eq. (3), the strain energy associated with the substitutional atom will take the form

$$E_{\text{strain}}(\text{AB:C}) = \frac{3}{2r_{0_{\text{AC}}}^2}\alpha_{\text{AC}}(r_{\text{AC}}^2 - r_{0_{\text{AC}}}^2)^2 + \frac{9}{2r_{0_{\text{AC}}}^2}\alpha_{\text{AB}}(r_{\text{AB}}^2 - r_{0_{\text{AB}}}^2)^2 + \text{bond bending terms}. \tag{A1}$$

The relaxation involves a balance between two opposing effects; adding the second-neighbor shell to the model reduces the relaxation, whereas introducing bond-bending terms increases the relaxation.[14] In the following, we neglect the bond-bending terms in order to cancel the error introduced by the restriction in the relaxation to the first neighbor shell.

Using the definition of ϵ in Eq. (9), one can rewrite the interatomic distances in terms of the strain and of the equilibrium spacing between atoms in the host crystal,

$$r_{\text{AC}} = r_{0_{\text{AB}}}(1+\epsilon), \tag{A2}$$

$$r_{\text{AB}} = r_{0_{\text{AB}}}\sqrt{1 - 2\epsilon/3 + \epsilon^2}. \tag{A3}$$

By substitution of Eqs. (A2) and (A3) to Eq. (A1), we obtain the strain energy as a function of ϵ. Expanding the result to a series of powers of ϵ and taking the derivative over ϵ, one obtains

$$\frac{dE_{\text{strain}}(\text{AB:C})}{d\epsilon} \approx 3\alpha_{\text{AC}}r_{0_{\text{AB}}}^4/r_{0_{\text{AC}}}^2 - 3\alpha_{\text{AC}}r_{0_{\text{AB}}}^2 + (2\alpha_{\text{AB}}r_{0_{\text{AB}}}^2 - 3\alpha_{\text{AC}}r_{0_{\text{AB}}}^2 + 9\alpha_{\text{AC}}r_{0_{\text{AB}}}^4/r_{0_{\text{AC}}}^2)\epsilon + \mathcal{O}[\epsilon^2]. \tag{A4}$$

The optimal value of ϵ, which minimizes the strain energy, can be obtained from $dE_{\text{strain}}/d\epsilon = 0$ that yields the simple result for the lattice distortion around isovalent substitutional impurity atom C placed in the sublattice B of the host AB zinc-blende lattice,

$$\epsilon \approx \frac{3\alpha_{\text{AC}}(r_{0_{\text{AC}}}^2 - r_{0_{\text{AB}}}^2)}{r_{0_{\text{AC}}}^2(2\alpha_{\text{AB}} - 3\alpha_{\text{AC}}) + 9r_{0_{\text{AB}}}^2\alpha_{\text{AC}}}. \tag{A5}$$

*oleg.rubel@physik.uni-marburg.de

[1] E. P. O'Reilly, Semicond. Sci. Technol. **4**, 121 (1989).
[2] I. Vurgaftman, J. R. Meyer, and L. R. Ram-Mohan, J. Appl. Phys. **89**, 5815 (2001).
[3] S. V. Dudiy and A. Zunger, Phys. Rev. Lett. **97**, 046401 (2006).
[4] P. M. Petroff, J. Vac. Sci. Technol. **14**, 973 (1977).
[5] N. Peranio, A. Rosenauer, D. Gerthsen, S. V. Sorokin, I. V. Sedova, and S. V. Ivanov, Phys. Rev. B **61**, 16015 (2000).
[6] W. Neumann, H. Kirmse, I. Häusler, R. Otto, and I. Hähnert, J. Alloys Compd. **382**, 2 (2004).
[7] H. Friedrich, M. McCartney, and P. Buseck, Ultramicroscopy **106**, 18 (2005).
[8] F. Glas, C. Gors, and P. Hénoc, Philos. Mag. B **62**, 373 (1990).
[9] F. Glas, Philos. Mag. **84**, 2055 (2004).
[10] K. Volz, O. Rubel, T. Torunski, S. D. Baranovskii, and W. Stolz, Appl. Phys. Lett. **88**, 081910 (2006).
[11] J. M. Zuo, J. C. H. Spence, and M. O'Keeffe, Phys. Rev. Lett. **61**, 353 (1988).
[12] A. Rosenauer, M. Schowalter, F. Glas, and D. Lamoen, Phys. Rev. B **72**, 085326 (2005).
[13] P. N. Keating, Phys. Rev. **145**, 637 (1966).
[14] J. L. Martins and A. Zunger, Phys. Rev. B **30**, 6217 (1984).
[15] T. Mattila and A. Zunger, J. Appl. Phys. **85**, 160 (1999).
[16] F. Grosse and J. Neugebauer, Phys. Rev. B **63**, 085207 (2001).
[17] *Crystal and Solid State Physics*, Landolt-Börnstein, New Series, Group III, Vol. III, edited by O. Madelung (Springer, Berlin, 1972).
[18] P. Blaha, K. Schwarz, G. K. H. Madsen, D. Kvasnicka, and J. Luitz, *WIEN2k: An Augmented Plane Wave Plus Local Orbitals Program for Calculating Crystal Properties* (Karlheinz Schwarz, Techische Universität, Wien, Austria, 2001).
[19] W. Kohn and L. J. Sham, Phys. Rev. **140**, A1133 (1965).
[20] A. F. Wright and J. S. Nelson, Phys. Rev. B **50**, 2159 (1994).
[21] H. J. Monkhorst and J. D. Pack, Phys. Rev. B **13**, 5188 (1976).
[22] N. F. Mott, Proc. R. Soc. London **A127**, 658 (1930).
[23] P. R. C. Kent and A. Zunger, Phys. Rev. B **64**, 115208 (2001).
[24] G. L. W. Hart and A. Zunger, Phys. Rev. B **62**, 13522 (2000).
[25] F. Glas, Phys. Rev. B **51**, 825 (1995).
[26] S.-G. Shen, J. Phys.: Condens. Matter **6**, 4449 (1994).
[27] D. B. Williams and C. B. Carter, *Transmission Electron Microscopy: A Textbook for Materials Science* (Plenum, New York, 1996).
[28] P. B. Hirsch, A. Howie, R. B. Nicholson, D. W. Pashley, and M. J. Whelan, *Electron Microscopy of Thin Crystals* (Butterworths, London, 1965).
[29] P. A. Stadelmann, Ultramicroscopy **21**, 131 (1987).
[30] L. Bellaiche, S. H. Wei, and A. Zunger, Phys. Rev. B **54**, 17568 (1996).
[31] P. A. Doyle and P. S. Turner, Acta Crystallogr., Sect. A: Cryst. Phys., Diffr., Theor. Gen. Crystallogr. **24**, 390 (1968).